ELSEVIER

Carbohydrate Polymers 52 (2003) 225–236

Carbohydrate Polymers

www.elsevier.com/locate/carbpol

Morphological characterization of the phase behavior of inulin–waxy maize starch systems in high moisture environments

J.E. Zimeri, J.L. Kokini*

Department of Food Science, Center for Advanced Food Technology, Cook College , Rutgers University, 65 Dudley Road, New Brunswick, NJ 08901-8529, USA

Received 1 July 2002; revised 12 September 2002; accepted 13 September 2002

Abstract

The morphological properties of mixed inulin–waxy maize starch (WMS) systems were characterized as a function of concentration. Macroscopically homogeneous samples were analyzed using light microscopy. Morphological findings were used to explain phase inversion behavior previously determined through rheological analysis. Inulin was labeled with fluorescein isothiocyanate in order to differentiate it from WMS. Fluorescence microscopy was used to characterize phase-separated systems, in which two phases with completely different morphologies co-existed: a WMS-rich phase with inulin crystallites embedded in an amorphous matrix, and an inulin-rich phase with inulin crystallites forming a continuous network. The mechanism of phase separation was determined to be that of nucleation and growth of inulin crystallites. Polarized light microscopy and differential scanning calorimetry were used to verify the crystalline nature of the inulin aggregates in the samples. A ternary phase diagram that summarizes the interactions between inulin and WMS at high moisture contents was generated.

Keywords: Inulin; Waxy maize starch; Fluorescence; Polarized light; Phase diagram

1. Introduction

Foods are commonly found as phase-separated systems, and thus, present a heterogeneous microstructure. Their properties are dependent on the phase separation processes. According to Tolstoguzov (2000), the morphology of heterophase food systems, adhesion between phases, and mechanical and other physical properties can be changed by food formulation, processing and texture modification. The incompatibility of food macromolecular compounds enables production of new, value-added, formulated foods (Tolstoguzov, 2000). Thus, strong interests in developing methods to characterize food phase behavior and in relating it to morphology and macroscopic properties exist.

Several studies have addressed mixed carbohydrate interactions, and it has been found that their miscibility in solution decreases with increasing concentration. For example, Kalichevsky, Orford, and Ring (1986) studied the phase behavior of aqueous solutions of dextran and amylose. At high dextran concentrations, polymer incompatibility and segregation of dextran-rich droplets reduced the firmness of the resulting mixed gel. Kalichevsky and Ring (1987) studied aqueous solutions of amylose and amylopectin. These polysaccharides were so similar chemically that immiscibility was expected to occur only at very high concentrations. However, even moderately concentrated aqueous solutions exhibited immiscibility due to the high molecular weight of amylopectin, which encouraged phase separation. Antonov, Pletenko, and Tolstoguzov (1987) used microscopy and ultracentrifugation to analyze phase-separated systems consisting of low concentrations of amylopectin mixed with water and hydrocolloids. German, Blumenfeld, Guenin, Yuryev, and Tolstoguzov (1992) studied the structure of systems containing amylose, amylopectin and their mixtures. A spontaneous decomposition into two coexisting phases occurred when an aqueous system of 1.5% amylose and 1.9% amylopectin was kept for 48 h at 85 °C. Amylopectin was considered as a precipitating agent since it reduced the thermodynamic quality of the solvent and facilitated the aggregation of amylose. An increase in the content of amylopectin resulted in changes in gel crystallinity and in

* Corresponding author. Tel.: +1-732-932-8306; fax: +1-732-932-8690.
E-mail address: kokini@aesop.rutgers.edu (J.L. Kokini).

0144-8617/03/$ - see front matter © 2003 Elsevier Science Ltd. All rights reserved.
PII: S0144-8617(02)00267-9

the mechanical-relaxation properties. Mohammed, Hember, Richardson, and Morris (1998) studied the co-gelation of agarose and waxy maize starch. Closs, Conde-Petit, Roberts, Tolstoguzov, and Escher (1999) investigated the phase separation of aqueous starch/galactomannan systems, summarizing the results in the form of a phase diagram. It was determined that the structural strength of the blends was greater than that of any of the individual components.

More recently, investigators have used fluorescence optical microscopy to investigate the microstructure of and interactions between polymers. As pointed out by Dibbern-Brunelli and Atvars (1995), recent applications of this analytical tool in polymer science include: '(1) determination of additive distribution in semi-crystalline polymers, (2) studies of morphology…and macromolecular interpenetration processes, and (3) miscibility in polymer blends.' For example, Heertje, Nederlof, Hendrickx, and Lucassen-Reynders (1990), documented the displacement of fluorescein isothiocyanate (FITC)-labeled sodium caseinate by monoacylglycerols and proteins from the interface of emulsions using confocal scanning laser microscopy (CSLM). Li, Sosnowski, Chaffey, Balke, and Winnik (1994) examined films composed of a mixture of poly(methyl methacrylate) (PMMA) and polystyrene (PS), in which the PMMA was labeled with a fluorescent dye. The morphology of the blends was characterized through CSLM and the broad distribution of small particles was attributed to phase separation by a nucleation and growth mechanism. Garnier, Schorsch, and Doublier (1995), investigated the phase separation in dextran/locust bean gum mixtures. The self-association of locust bean gum was confirmed by fluorescence microscopy using FITC-labeled dextran. Dibbern-Brunelli and Atvars (1995); Dibbern-Brunelli, Atvars, Joekes, and Barbosa (1998) studied mixtures of poly(vinyl alcohol)/poly(vinyl acetate) using fluorescence microscopy, being able to chemically discriminate between each domain in phase-separated systems by observing the distribution of molecular probes. Blonk, van Eendenburg, Koning, Weisenborn, and Winkel (1995) studied aqueous mixtures of fluorescently labeled sodium caseinate and sodium alginate using CSLM. Estimation of the relative volumes of the phases through quantification of the intensity level of the fluorescent phases gave similar results than those obtained with classical gravimetric methods (via ultracentrifugation) for microscopically phase-separated systems. Goff, Ferdinando, and Schorsch (1999) investigated the structure of locust bean and guar gum in frozen sucrose and milk protein solutions using fluorescence microscopy, and confirmed that both compounds promoted the formation of a phase-separated protein region. In 2000, Sengupta et al. studied the phase separation of α-casein/β-casein/water at the air–water interface using fluorescence microscopy. Although these compounds belonged to the same class of proteins and had a similar molecular weight (~24,000), they were significantly different in terms of their structural and charge characteristics.

Polarized light microscopy is another optical technique, which is used to differentiate between crystals and amorphous material. A material is birefringent if plane polarized light travels through it at a different speed, depending on the angle of the plane relative to an axis on the material face. Birefringence measures the difference in the speed of light for two perpendicularly plane polarized beams (Bonnecaze & Brady, 1992). This technique is typically used to investigate the physical state of starch granules, which in the crystalline state are characterized by the presence of a Maltese cross pattern. Loss of birefringence is an indication of the irreversible swelling of starch granules that occurs above the gelatinization temperature (Aguilera & Stanley, 1999). For example, Bhatnagar and Hanna (1996) used polarized light microscopy to determine starch gelatinization in single-screw and twin-screw extruders. Bryant and Hamaker (1997) used polarized light hot-stage microscopy to monitor the onset and final temperatures of gelatinization of corn starch and defatted corn flour samples. Koch and Jane (2000) determined the morphological changes in granules of different starches by surface gelatinization with calcium chloride, using polarized light microscopy. This technique has also been used to investigate the crystallization and melting behavior of synthetic polymers, as in the case of Pizzoli, Scandola, and Ceccorulli (2002) who studied systems of poly (3-hydroxybutyrate) in the presence of a low molecular weight diluent.

Among the biopolymers that are being used as fat replacers in foods, inulin, a fructooligosaccharide, is used either as a macronutrient substitute to replace fat or as a supplement added mainly for its nutritional properties (Niness, 1999; Schaller-Povolny & Smith, 1999). Although its nutritional properties have been thoroughly studied (Roberfroid, Gibson, & Delzenne, 1993; Roberfroid, 1999a, b, 2000), inulin's physicochemical properties and interactions with other food biopolymers have just begun to be characterized. In previous studies, the authors determined that: (a) native inulin presented characteristics of a semi-crystalline material. When pre-solubilized, dried and stored at low moisture contents, concentrated samples of inulin presented a low relative crystallinity (~13%). When stored at conditions above T_g ($a_w > 0.75$), it recrystallized and reached native inulin's crystallinity level (~42%) (Zimeri & Kokini, 2002a). (b) Concentrated mixed samples of inulin–waxy maize starch (WMS) presented two individual T_g's, which corresponded to those of the individual components, evidence of a lack of interaction between them. Thus, it was concluded that phase separation had occurred (Zimeri & Kokini, 2003a). (c) At high moisture contents (≥60% w/w), a change in the rheological properties (steady shear, dynamic and relaxation data) of mixed inulin–WMS gels indicated that a phase inversion had occurred when the samples changed from a WMS-continuous system with inulin as the dispersed phase, to an inulin-continuous system with WMS as the dispersed

phase. Above c^*, limiting concentration between dilute and semi-dilute polymeric solutions, inulin formed strong gels (Zimeri & Kokini, 2003b).

The objectives of the present study were: (a) to determine the morphological changes (microstructure and crystallinity properties) caused by changes in concentration in mixed inulin–WMS systems at high moisture contents, and (b) to develop a phase diagram which relates the phase behavior of these biopolymers to composition.

2. Materials and methods

2.1. Sample preparation

Inulin (Raftiline® HP, >99.5% pure, donated by Orafti, Malvern, PA), waxy maize starch (98% amylopectin, obtained as Amioca™ from National Starch, Bridgewater, NJ) and mixtures were prepared in the following total polymer concentrations (w/w, w.b.): 2, 5, 10, 20, 30 and 40%, at ratios of inulin to WMS of 0:10, 25:75, 50:50, 75:25 and 10:0. Powders were mixed and dispersed in deionized water in a Helmco–Lacy waterproof hot cup (Star Mfg. Co., St Louis, MO). The cup was connected to a variable autotransformer (Powerstat, The Superior Electric Co., Bristol, CT), which allowed for heating rate regulation; a high heating rate minimized moisture loss while preparing the samples. Temperature was measured with a thermometer. Mixing was provided via a propeller, attached to a mixer (Model LR-41A, Yamato, Japan), operated at a speed of 350 rpm. In order for a good blending to occur, samples were further mixed using a stir plate at 90 °C for 30 min. Using aluminum foil to cover the samples prevented moisture evaporation. Samples were cooled down at room temperature and stored for 24 h previous to analysis to avoid the presence of bubbles formed during heating and mixing.

2.2. Visual analysis

Visual observations of the physical state of the samples (phase-separated or not) were recorded as digital pictures after the samples had reached an equilibrium state, after which no more changes were macroscopically observed. This period consisted of 24 h for most of the samples, and up to 3 weeks for samples that presented syneresis, as will be discussed later.

2.3. Fluorescence microscopy

Inulin was covalently labeled with fluorescein isothiocyanate (FITC, Lot 61K5317, Sigma Chemical Co., St Louis, MO) following the procedure described by DeBelder and Granath (1973), which was modified by substituting dextran by inulin. 1 g of inulin was dissolved in 10 ml dimethyl sulphoxide (DMSO) containing a few drops of pyridine. 0.1 g of FITC was added, followed by 20 mg of dibutylin dilaurate (used as a catalyst). The mixture was heated for 2 h at 95 °C using a stirring hot plate. Several precipitations in ethanol were performed to remove the free dye. FITC-inulin was filtered using a filter paper No. 3 (Whatman, W and R Balston Ltd, England), dried overnight in a vacuum oven at 80 °C, and stored under refrigeration and away from light to prevent degradation. DeBelder and Granath (1973) reported a degree of substitution of dextran with FITC of 0.001, which should not affect the viscosity of the labeled polysaccharides in solution compared to before labeling.

In order to prepare mixed inulin–WMS samples, 1% of the total inulin was replaced by FITC-inulin before heating. The sample preparation procedure outlined above was followed. After a storage time of 24 h at room temperature, samples were placed in slides with a cover slip and were immediately observed (to prevent dehydration) at magnifications of 40X under a fluorescence microscope (Olympus, Japan) equipped with a mercury lamp (CHIU Tech. Corp, NY), exciter/emission filters and a digital camera (CRI, MA). Light and fluorescence photomicrographs of the samples were acquired.

2.4. Polarized light microscopy

After 24 h of storage at room temperature, samples were placed in slides with a cover slip and were immediately observed (to avoid dehydration) at a magnification of 40X under a polarized light microscope (Model BX60 F-3, Olympus, Japan). Photomicrographs were acquired with a digital camera (Model DEI-750, Optronics Engineering, USA).

2.5. Differential scanning calorimetry (DSC)

Experiments were conducted on a TA-4000 Differential Scanning Calorimeter (Mettler-Toledo, Columbus, OH) at a heating rate of 10 °C/min. Calibration of the instrument was performed using indium as a standard. Hermetic medium pressure pans were used to avoid moisture loss during analysis. Measurements were performed at least in duplicate and an empty pan was used as reference. Melting of crystalline materials, a first order phase transition, was observed as an endothermic peak on DSC thermograms.

3. Results and discussion

3.1. Visual observation of macroscopic behavior

Mixed inulin and WMS samples appeared homogeneous with no signs of phase separation immediately after mixing and heating. After the samples reached equilibrium, different behaviors were observed, depending on the composition. Macroscopically, monophasic behavior was prevalent in either: (a) pure WMS suspensions, (b) mixed

gels at 2 and 5% total polymer concentrations, in which inulin concentration was ≤50% of the polymers, or (c) samples with total polymer concentrations ≥20%, in which inulin constituted 75 or 100% of the polymers. Otherwise, samples presented biphasic behavior due to: (a) syneresis, as mentioned by Zimeri and Kokini (2003b), in which either inulin or WMS were below c^* (limiting concentration between a dilute and a semi-dilute solution (Carriere, 1998)); and (b) existence of two gels in one system, in which an opaque phase was dispersed within a more transparent, continuous phase. The last scenario confirmed the incompatibility between the two biopolymers, previously observed by Zimeri and Kokini (2003a) in samples under limited moisture environments.

3.2. Light microscopy

Samples were analyzed using light microscopy after 24 h of storage. Fig. 1 shows the light micrographs of macroscopically homogeneous samples at 5% total polymer concentration, at inulin to WMS ratios of (a) 0:10 (pure WMS); (b) 25:75; (c) 50:50 and (d) 10:0 (pure inulin), observed at 40X magnification. Fig. 1(a)–(c) present the morphological differences between samples in which WMS went from concentrated (Fig. 1(a)) to semi-dilute (Fig. 1(b) and (c)) systems; as inulin concentration increased, the samples became more dilute, as determined by Zimeri and Kokini (2003b). A few starch granule remnants were present in the more concentrated samples, and disappeared at lower WMS concentrations. According to Rolee and Le Meste (1997), waxy corn starch has a granular size of 5–25 μm. It is known that when starch granules are heated in water, the granules take up available water, and the loss of crystallinity is progressive. At intermediate states of heating or in limited water, some crystallinity persists (Jacobs & Delcour, 1998; Stauffer, 2000). The temperature at which starch gelatinizes depends on the amount of water available. At least two parts water to one part starch by weight are needed for all starch to gelatinize in the normal temperature range (about 60–70 °C) (Stauffer, 2000). If the water–starch ratio is lower, the temperature necessary to complete gelatinization is higher, since the remaining crystalline portion melts during an anhydrous process that occurs over a temperature range of up to 115 °C (Stauffer, 2000). At these concentrations, Zimeri and Kokini (2003b) determined that the samples presented rheological characteristics of weak gels.

Fig. 1(d) (5% pure inulin) shows the presence of some inulin crystals immersed in a continuous medium. This sample had not reached equilibrium after 24 h, since sedimentation occurred after 3 weeks of storage at room temperature. Inulin's solubility in water depends on temperature, and at 90 °C, it has been reported to be about 35% (Silva, 1996). Thus, the remaining crystals could have been the result of either insolubility or recrystallization after hot inulin dispersions were cooled to room temperature (Zimeri & Kokini, 2002). At this concentration, inulin was found below its c^* and showed dilute solution rheological behavior (Zimeri & Kokini, 2003b).

In comparison, Fig. 2 presents light micrographs (40X) of more concentrated, macroscopically homogeneous gels. In Fig. 2(a) (30% 0:10, pure WMS), it is evident that starch granules and granule remnants (10–25 μm) were dispersed throughout a continuous matrix, forming a gel. A starch gel can be viewed as a composite, in which deformable gelatinized granules are embedded and reinforce a continuous matrix (Biliaderis, 1991). Fig. 2(b) (30% 10:0, pure inulin) presents the morphology of inulin samples at the same concentration as that of WMS in Fig. 2(a). At this concentration, inulin shows a microstructure formed by clusters of small inulin crystals of 10 μm in diameter. If Fig. 1(d) is compared to Fig. 2(b), the transition from dilute to concentrated inulin samples can be visualized. These results are complemented by findings by Hébette et al. (1998), who studied the melting behavior of semi-crystalline chicory root inulin. Concentrated solutions (30–45% w/w) of inulin (d.p. = 12) were prepared and cooled from 96 to 20 °C, finding that suspensions of semi-crystalline material in water were formed. Large 8-like shaped crystallites resulted from primary nucleation at higher temperature and smaller 8-like shaped crystallites resulted from secondary nucleation at lower temperature.

Samples at an inulin to WMS ratio of 75:25 at concentrations of 30 and 40% are presented in Fig. 2(c) and (d), respectively. In Fig. 2(c), the mixed system presented a highly aggregated microstructure, with particles ranging between 10 and 100 μm. In comparison, Fig. 2(d) presented a more uniform structure formed by densely packed, homogeneously sized crystallites (10 μm), with an appearance very similar to that of pure inulin (Fig. 2(b)). The differences in particle sizes between Fig. 2(c) and (d) can probably be attributed to differences in inulin diffusion, which was facilitated by a lower viscosity at 30%, thus being able to form larger crystalline aggregates. A higher inulin content shown in Fig. 2(d) facilitated the agglomeration into a densely packed structure. These micrographs can be used to complement findings by Zimeri and Kokini (2003b), who determined that a change in rheological properties was observed in samples at 30% 75:25, compared to samples with lower inulin content. From this inulin concentration up, the moduli's magnitude increased with the addition of inulin, and samples showed a strong gel behavior. Phase inversion from a WMS-continuous system (at lower inulin concentrations) to an inulin-continuous system was caused by inulin forming strong gels at concentrations above c^*, as observed in Fig. 2(c) and (d). At 40%, inulin presented strong gel rheological behavior (Zimeri & Kokini, 2003b) and formed a continuous network, as observed in Fig. 2(d).

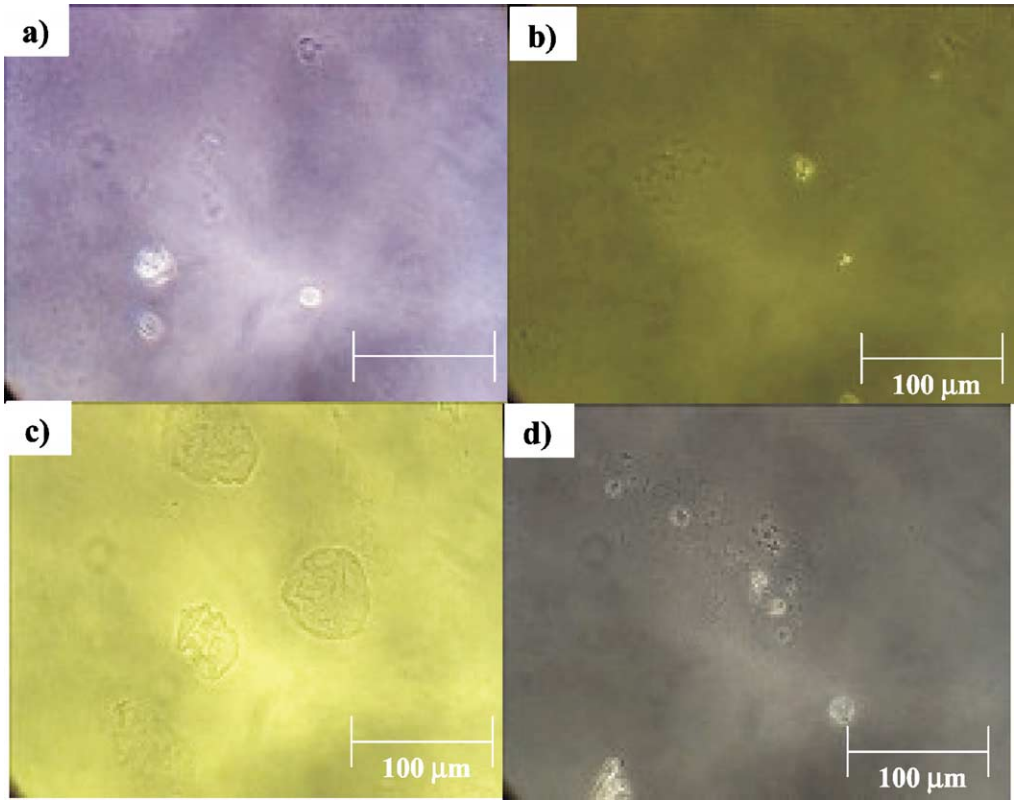

Fig. 1. Light micrographs of homogeneous samples at 5%, total polymer concentration, inulin to WMS ratios of: (a) 0:10, (b) 25:75, (c) 50:50 and (d) 10:0.* (40X). *Before sedimentation occurred.

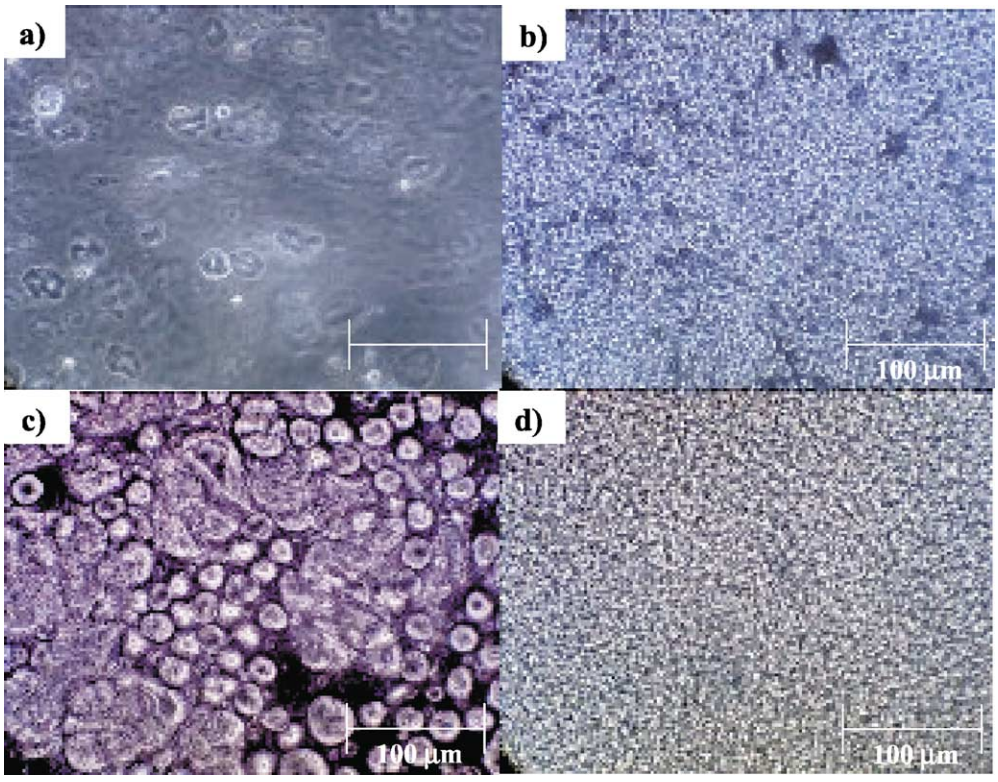

Fig. 2. Light micrographs of homogeneous samples at 30% total polymer concentration, inulin to WMS ratios of: (a) 0:10 and (b) 10:0; homogeneous samples at inulin to WMS ratio of 75:25, total polymer concentrations of: (c) 30% and (d) 40%. (40X).

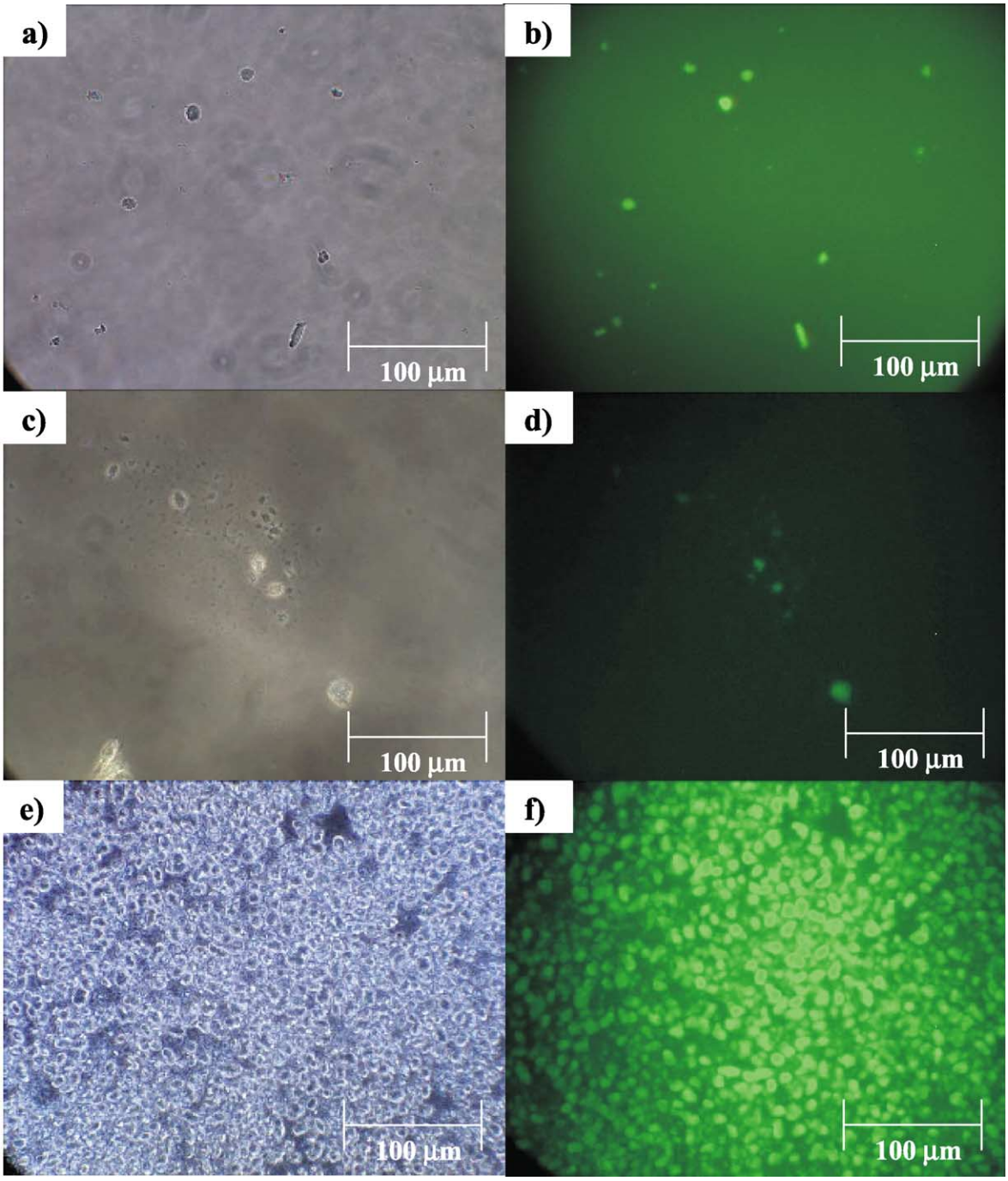

Fig. 3. Inulin samples at concentrations of (a) and (b) 2%*; (c) and (d) 5%*; (e) and (f) 30%; viewed under light and fluorescence microscopy, respectively. (40X). *Before sedimentation occurred.

3.3. Fluorescence microscopy

Up to this point, a differentiation between inulin and WMS particles was not possible, since both compounds had similar dimensions when in the crystalline form. When observed under a fluorescence microscope, both inulin and WMS presented a diffuse, green-emitting intrinsic fluorescence, which in the case of WMS was adjudicated to extraneous, non-granular material, after observation under a polarized light microscope. Autofluorescence was weak and faded when exposed to light, as suggested in the literature (Aguilera & Stanley, 1999). Thus, to ensure intense emissions, inulin was labeled with FITC to differentiate it from WMS. Micrographs of FITC-inulin (10:0) are shown in Fig. 3 as a function of total concentration, observed under light and fluorescence microscopy at a magnification of 40X, as follows: (a) 2% light, (b) 2% fluorescence, (c) 5% light, (d) 5% fluorescence, (e) 30% light, and (f) 30% fluorescence. It should be mentioned that 2 and 5% samples were photographed after 24 h, before reaching an

equilibrium state in which sedimentation occurred. At 2 and 5% concentrations, inulin did not form a continuous phase, since its concentration was under c^* (Zimeri & Kokini, 2003b). As inulin's concentration increased to 30% (Fig. 3(e) and (f)), small crystallites ~10 μm in diameter were observed. As Zimeri and Kokini (2003b) concluded from rheological measurements, at this concentration pure inulin samples presented a 'liquid-like' behavior, although the moduli reached a high magnitude (10^4 dyn/cm^2). This behavior was explained by the hypothesis of inulin's structure corresponding to one with no entanglements at all, with agglomerates (crystals) sliding one on top of the other. Fig. 3(e) and (f) confirm this hypothesis as seen from the presence of small inulin crystallites throughout the sample, with no interconnections with one another.

Samples that presented macromolecular phase separation were also analyzed using fluorescence microscopy. Both phases presented dissimilar characteristics, since one of them was more elastic and transparent, and the other one was more rigid and opaque. To illustrate these results, Fig. 4 presents micrographs (40X) of both phases, analyzed separately, for a sample with a 30% 25:75 composition. Light regions represent fluorescent inulin (observed as green under the microscope) and dark regions represent non-fluorescent domains. Fluorescent domains can be attributed to those richer in inulin, and dark to those richer in WMS. Fig. 4(a) and (b) show micrographs of the transparent phase observed under light and fluorescence microscopy, respectively. A few number of large inulin aggregates (spherulites) were suspended in WMS. Their large diameter (40 μm) indicated that crystal size probably reached this large dimension due to inulin diffusion within this phase. A WMS-continuous system gave a transparent appearance to this phase. In comparison, Fig. 4(c) and (d) present micrographs of the opaque phase, observed under light and fluorescence microscopy, respectively. In this case, the appearance was very similar to that of pure inulin, with small crystallite clusters present throughout the inulin-rich phase, which conferred it the opaque appearance. The small size of the crystallites was caused by a concentrated inulin phase, which facilitated nucleation. Thus, two phases with completely different morphologies confirmed the presence of separated networks and the existence of phase separation. Zimeri and Kokini (2003b) indicated that at this concentration, samples showed rheological characteristics of a weak gel. Both components probably gelled independently, with WMS remaining in the amorphous state (Zimeri & Kokini, 2003a) and inulin recrystallizing (Zimeri & Kokini, 2002).

Phase-separated samples at 30% 50:50 concentration were examined in a similar manner. The WMS-rich phase is presented in Fig. 5(a) and (b) (40X magnification) under light and fluorescence microscopy, respectively. In this case, crystallites were bigger in size (60 μm) than those shown in Fig. 4 due to higher concentration of inulin to form the crystalline aggregates in the WMS-continuous phase, facilitated by diffusion. Micrographs of the inulin-rich phase are shown in Fig. 5(c) and (d) under light and fluorescence microscopy, respectively. Inulin formed aggregates ranging from 10 to 60 μm in diameter. Thus, due to a high inulin concentration, smaller crystals were packed into clusters as a result of a high nucleation rate within this phase. Zimeri and Kokini (2003b) indicated that the overall rheological properties of this sample presented a decrease in the moduli's magnitude due to WMS network disruption by inulin, when compared to gels with lower inulin concentrations. Thus, as the degree of phase separation was greater, and inulin content increased, the overall structure of the gel became weaker.

Fig. 6 shows micrographs (40X magnification) of phase-separated gels at 40% 25:75 concentration. Again, the WMS-rich phase was observed under light (Fig. 6(a)) and fluorescence microscopy (Fig. 6(b)). This phase presented a bimodal distribution of inulin spherulites of 80 and 30 μm in diameter, larger than those found in 30% samples, indicating that smaller spherulites had aggregated to form the large ones, in spite of a higher viscosity than at 30% inulin. The inulin-rich phase observed under light (Fig. 6(c)) and fluorescence microscopy (Fig. 6(d)) was formed by closely packed inulin crystallites that formed a continuous network. Relating these results to rheological properties (Zimeri & Kokini, 2003b), it was found that from this concentration up, keeping the total polymer concentration to 40%, the moduli's magnitude increased with inulin content, indicating that the gels became stronger as more inulin was added.

According to Fabri, Guan, and Cesàro (1998), segregation of the polymer chains in two domains with different concentrations is the selective rule for the occurrence of two ordered microphases. Since in the present case both phases contained both biopolymers, total phase separation was not achieved due to the gelation of WMS. Total diffusion of inulin was prevented by the formation of a starch network and by the resulting high viscosity.

Similarly to results determined by Li et al. (1994) for other polymer systems, a mechanism for the phase separation process at high moisture contents can be suggested for inulin–WMS systems based on morphological results: phase separation by nucleation and growth produces a dispersion of spheres of the minor component (inulin) in the major component matrix (WMS) with a broad distribution of particle sizes. The spherical shape is a consequence of surface energy minimization within each particle. As inulin crystallizes, the system passes into a two-phase region and begins to demix. The final morphology will be determined by the rate of crystallization and diffusion (regulated by viscosity). Similarly, Sengupta, Razumovsky, and Damodaran (2000) stated that, when examining α- and β-casein mixtures by fluorescence microscopy, separation into phases was kinetically limited by the viscosity barrier to diffusion of the molecules. The phase separation process described above can be

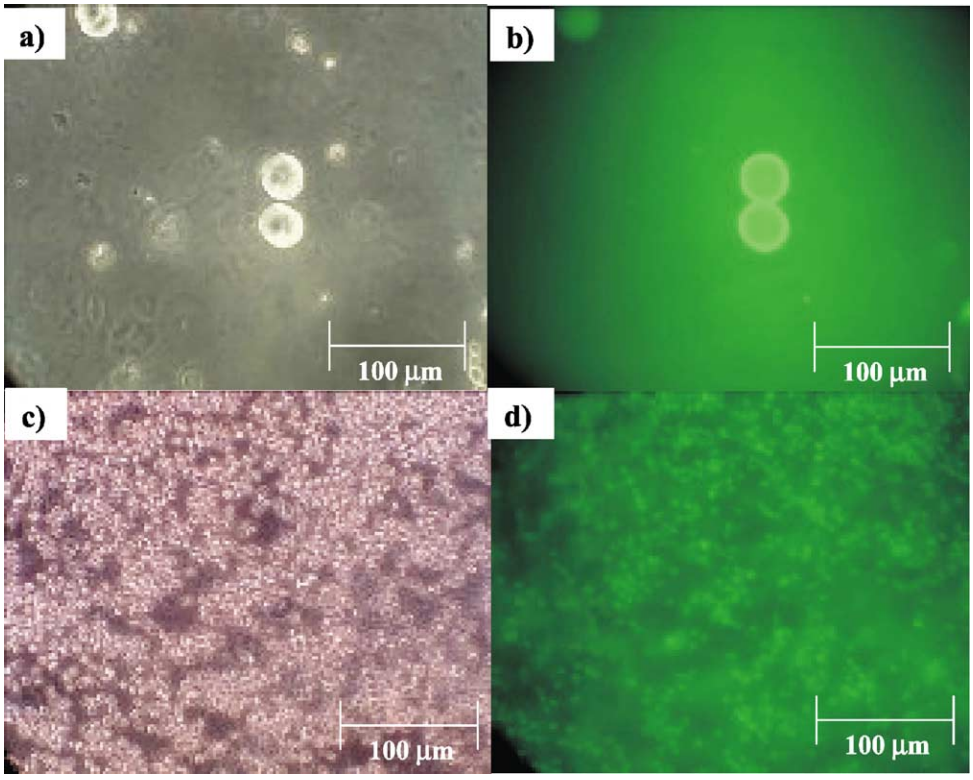

Fig. 4. Micrographs of a phase-separated sample at 30% total polymer concentration, inulin to WMS ratio of 25:75. WMS-rich phase viewed under (a) light, (b) fluorescence microscopy; inulin-rich phase viewed under (c) light, (d) fluorescence microscopy. (40X).

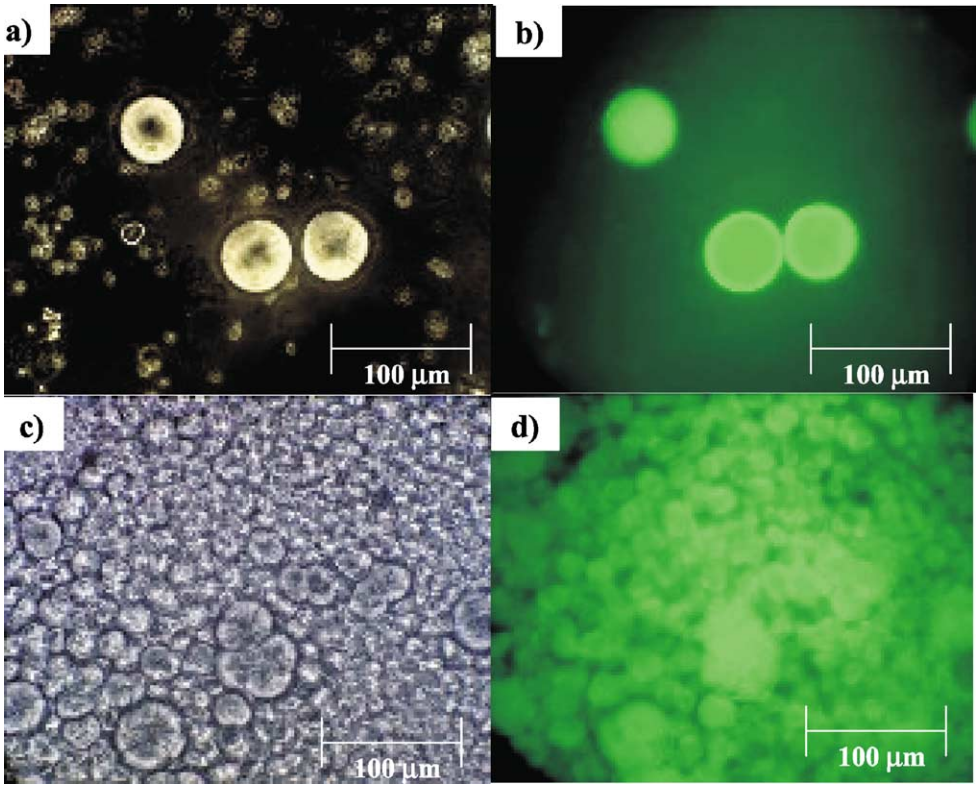

Fig. 5. Micrographs of a phase-separated sample at 30% total polymer concentration, inulin to WMS ratio of 50:50. WMS-rich phase viewed under (a) light, (b) fluorescence microscopy; inulin-rich phase viewed under (c) light, (d) fluorescence microscopy. (40X).

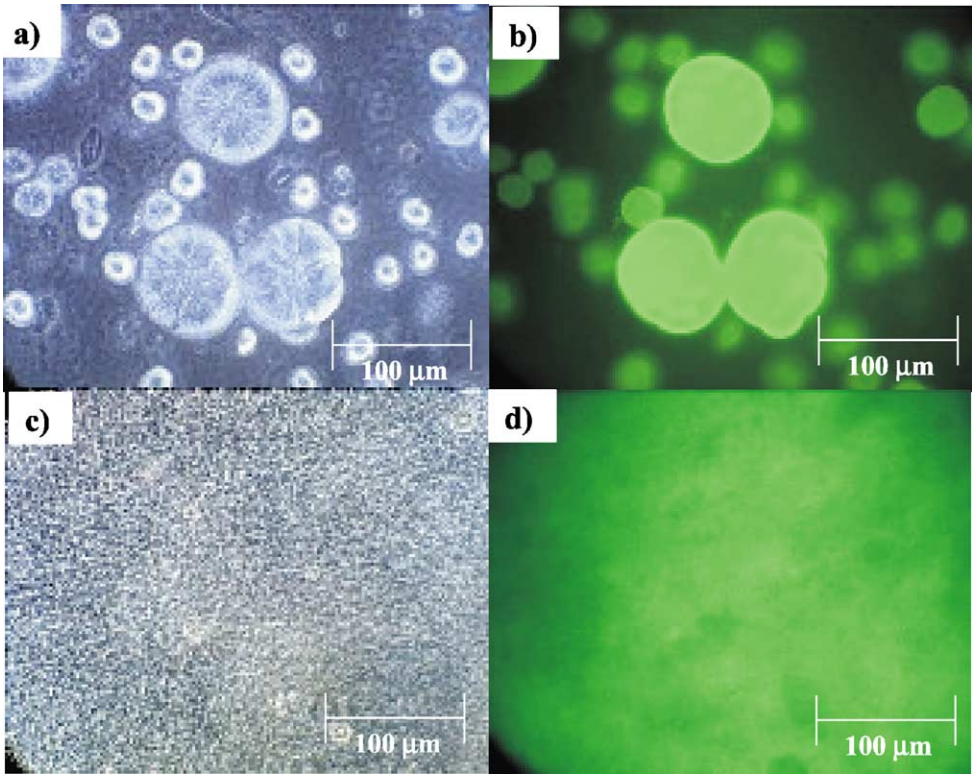

Fig. 6. Micrographs of a phase-separated sample at 40% total polymer concentration, inulin to WMS ratio of 25:75. WMS-rich phase viewed under (a) light, (b) fluorescence microscopy; inulin-rich phase viewed under (c) light, (d) fluorescence microscopy. (40X).

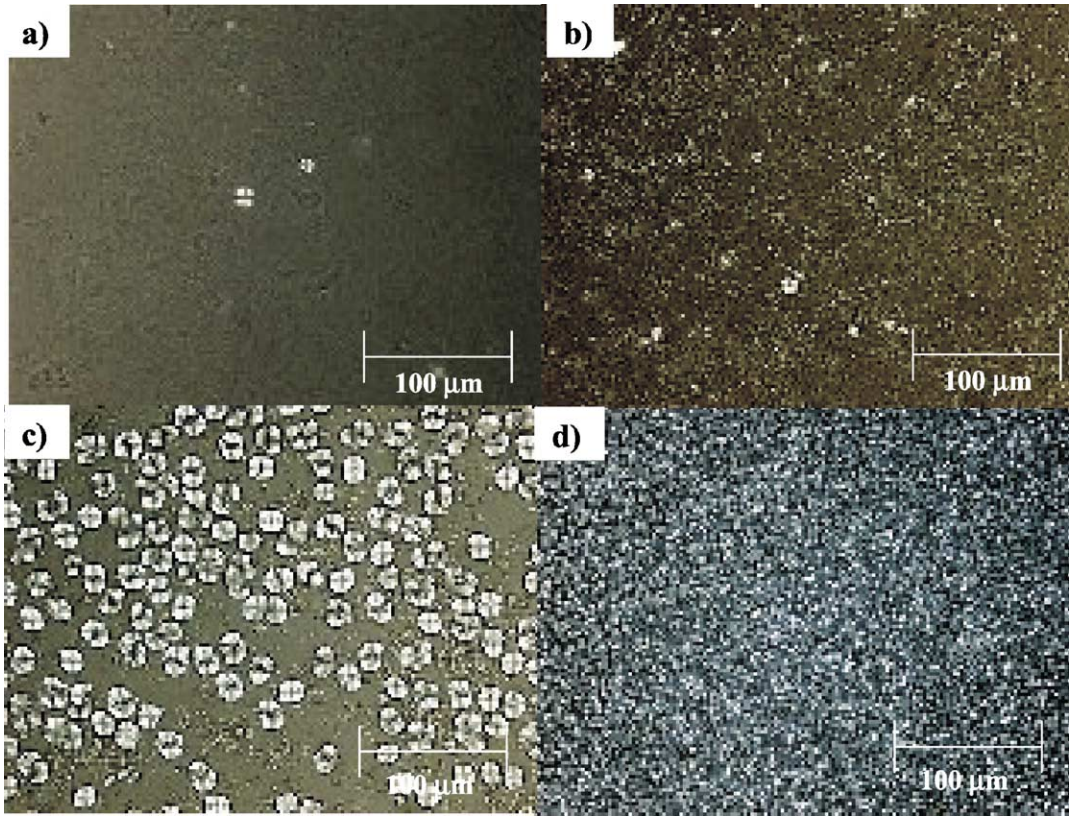

Fig. 7. Polarized light micrographs of samples at 30% total polymer concentration, at inulin to WMS ratios of: (a) 0:10; (b) 25:75; (c) 75:25 and (d) 10:0. (40X).

differentiated from spinodal decomposition, which initially leads to a bicontinuous network that eventually breaks up into droplets, resulting in periodicity in drop formation and a more uniform droplet size (Li et al., 1994).

3.4. Polarized light microscopy

In order to confirm the crystalline nature of the observed aggregates, samples were observed under a polarized light microscope. Fig. 7 presents micrographs of samples with the following compositions (40X): (a) 30% 0:10 pure WMS, in which a few starch granules and mostly granule remnants were present. A Maltese cross-like pattern was observed, indicating the existence of uniaxial crystals. As indicated by Stauffer (2000), at intermediate states of heating or in situations where water is limited, some birefringence persists; (b) 30% 25:75, inulin-rich phase; (c) 30% 75:25, homogeneous sample, no phase separation observed; and (d) 30% 10:0, pure inulin. When these micrographs are compared to those obtained by fluorescence microscopy, it can be concluded that fluorescent inulin aggregates effectively corresponded to crystallites. As indicated by Hébette et al. (1998) inulin has been found to be a crystalline solid in the native state, and after dispersion in water, it recrystallizes (Zimeri & Kokini, 2002). Thus, as inulin content increased, the crystallinity of the gels increased. And when inulin was able to form a continuous network (above c^*), strong crystalline gels formed.

3.5. Differential scanning calorimetry

Changes in crystallinity with increasing inulin concentration were also investigated through DSC analysis. The thermogram for the WMS-rich phase of a 30% 50:50 sample is shown in Fig. 8(a). Small endotherms indicated a low degree of crystallinity, as expected from a low inulin content (Fig. 5(a) and (b)) and from WMS slow recrystallization rate at the studied concentrations (Liu & Thompson, 1998). As inulin concentration increased to 30% 75:25, the system shifted towards a macroscopically homogeneous state with increased crystallinity (Fig. 8(b)), where a clear endotherm was present at inulin's dissolution temperature (~80 °C). Similar results were described by Hébette et al. (1998) who obtained DSC thermograms for inulin that displayed melting profiles with three to four partly overlapping endotherms that varied as a function of concentration, cooling rate during crystallization and storage time at 25 °C of the crystallite suspension. A bimodal distribution of crystal size could result in multiple melting peaks due to different fractions of crystallinity (Fabri et al., 1998).

3.6. Ternary phase diagram

A phase diagram for a ternary system consisting of WMS, inulin and water was created, based on the information generated on this and a previous publication (Zimeri & Kokini, 2003b), and is shown in Fig. 9. The shaded areas correspond to those in which monophasic behavior was observed. The system was bi-phasic when a WMS-rich phase formed the continuous network, in which an inulin-rich phase was dispersed. As soon as inulin's concentration reached c^*, it formed a continuous, crystalline phase, presenting characteristics

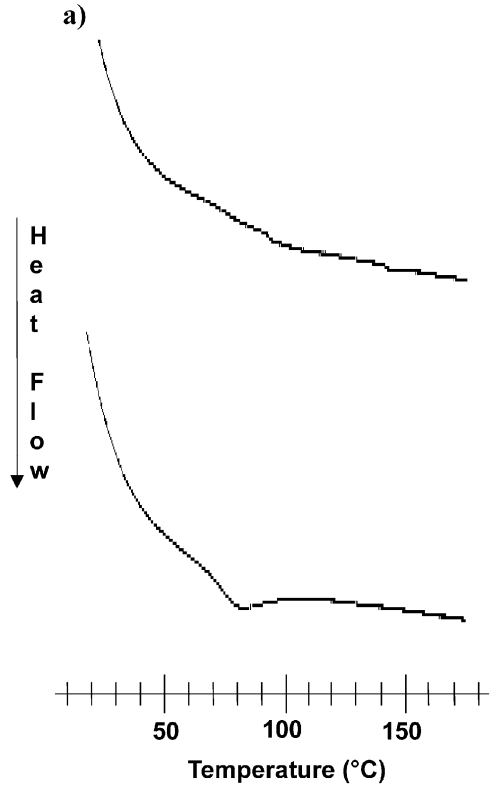

Fig. 8. DSC thermograms of samples at 30% total polymer concentration at inulin to WMS ratios of: (a) 50:50 and (b) 75:25.

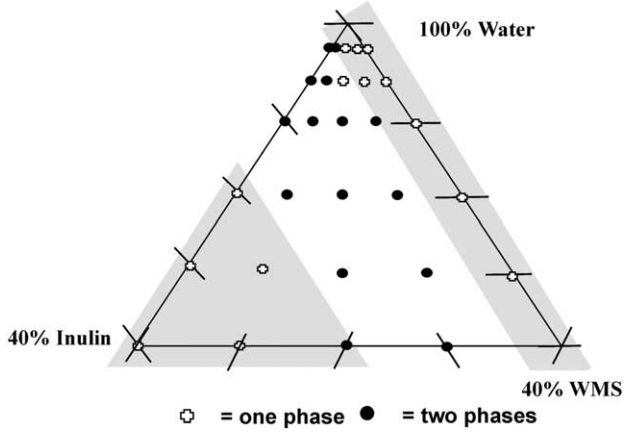

Fig. 9. Phase diagram of a ternary system constituted by WMS and inulin at high moisture contents (≥60%).

of a one-phase system. This phase diagram can be used to predict the behavior of the two carbohydrates in foods at high moisture contents, and more specifically, inulin's functionality as a fat replacer.

4. Conclusions

Macroscopically homogeneous systems ranged from semi-dilute samples in which WMS granules, granule remnants and inulin crystals, formed weak gels, to mixed systems with a highly aggregated, crystalline microstructure. Phase inversion phenomena observed through rheological analysis of the mixed samples (Zimeri & Kokini 2003b), caused by inulin forming strong gels above c^*, could be visualized through light and fluorescence microscopy. Phase-separation was confirmed by the existence of two phases with completely different morphologies: a WMS-rich phase with inulin crystallites embedded in an amorphous matrix, and an inulin-rich phase with inulin crystallites forming a continuous network. Phase-separation contributed to the weak gel rheological behavior of the samples, characterized in a previous study (Zimeri & Kokini, 2003b). Nucleation and growth were the suggested mechanisms responsible for phase separation at high moisture contents. The final morphology was then determined by the rate of crystallization and diffusion (regulated by viscosity) of the components that formed microstructure domains, whose dimensions and distributions were dependent on the composition of the mixed gels. Phase behavior was captured in the form of a ternary phase diagram which describes the interactions between inulin, WMS and water.

Acknowledgements

This is publication No. D-10544-5-02 of the New Jersey Agricultural Experiment Station supported by State Funds and the Center for Advanced Food Technology (CAFT). The Center for Advanced Food Technology is a New Jersey Commission on Science and Technology Center. The authors would like to thank National Starch (Bridgewater, NJ) for letting them use their polarized light microscope, and Orafti (Malvern, PA) for donating the inulin which was used in this and previous studies.

References

Aguilera, J. M., & Stanley, D. W. (1999). Examining food microstructure. In J. M. Aguilera, & D. W. Stanley (Eds.), *Microstructural principles of food processing and engineering* (pp. 1–70). Aspen Publications.

Antonov, Y. A., Pletenko, M. B., & Tolstoguzov, V. B. (1987). Phase state of the systems water–polysaccharide-I–polysaccharide-II. *Polymer Science USSR (Vysokomol. Soyed.)*, *29*(12), 2724–2729.

Bhatnagar, A., & Hanna, M. A. (1996). Starch–stearic acid complex development within single and twin screw extruders. *Journal of Food Science*, *61*(4), 778–782.

Biliaderis, C. G. (1991). The structure and interactions of starch with food constituents. *Canadian Journal of Physiology and Pharmacology*, *69*, 60–78.

Blonk, J. D. G., van Eendenburg, J., Koning, M. M. G., Weisenborn, P. C. M., & Winkel, C. (1995). A new CSLM-based method for determination of the phase behaviour of aqueous mixtures of biopolymers. *Carbohydrate Polymers*, *28*, 287–295.

Bonnecaze, R. T., & Brady, J. F. (1992). Yield stresses in electrorheological fluids. *Journal of Rheology*, *36*(1), 73–115.

Bryant, C. M., & Hamaker, B. R. (1997). Effect of lime on gelatinization of corn flour and starch. *Cereal Chemistry*, *74*(2), 171–175.

Carriere, C. J. (1998). Evaluation of the entanglement molecular weights of maize starches from solution rheological measurements. *Cereal Chemistry*, *75*(3), 360–364.

Closs, C. B., Conde-Petit, B., Roberts, I. D., Tolstoguzov, V. B., & Escher, F. (1999). Phase separation and rheology of aqueous starch/galactomannan systems. *Carbohydrate Polymers*, *39*, 67–77.

DeBelder, A. N., & Granath, K. (1973). Preparation and properties of fluorescein-labeled dextrans. *Carbohydrate Research*, *30*, 375–378.

Dibbern-Brunelli, D., & Atvars, T. D. Z. (1995). In situ chemical analysis of domains in polymer blends by optical fluorescence microscopy. *Journal of Applied Polymer Science*, *58*, 779–786.

Dibbern-Brunelli, D., Atvars, T. D. Z., Joekes, I., & Barbosa, V. C. (1998). Mapping phases of poly(vinyl alcohol) and poly(vinyl acetate) blends by FTIR microspectroscopy and optical fluorescence microscopy. *Journal of Applied Polymer Science*, *69*, 645–655.

Fabri, D., Guan, J., & Cesàro, A. (1998). Crystallisation and melting behaviour of poly (3-hydroxybutyrate) in dilute solution: Towards an understanding of physical gels. *Thermochimica Acta*, *321*, 3–16.

Garnier, C., Schorsch, C., & Doublier, J. L. (1995). Phase separation in dextran/locust bean gum mixtures. *Carbohydrate Polymers*, *28*, 313–317.

German, M. L., Blumenfeld, A. L., Guenin, Ya. V., Yuryev, V. P., & Tolstoguzov, V. B. (1992). Structure formation in systems containing amylose, amylopectin, and their mixtures. *Carbohydrate Polymers*, *18*, 27–34.

Goff, H. D., Ferdinando, D., & Schorsch, C. (1999). Fluorescence microscopy to study galactomannan structure in frozen sucrose and milk protein solutions. *Food Hydrocolloids*, *13*, 353–362.

Hébette, C. L. M., Delcour, J. A., Koch, M. H. J., Booten, K., Kleppinger, R., Mischenko, N., & Reynaers, H. (1998). Complex melting of semi-crystalline chicory (*Cichorium intybus* L.) root inulin. *Carbohydrate Research*, *310*, 65–75.

Heertje, I., Nederlof, J., Hendrickx, H. A. C. M., & Lucassen-Reynders, E. H. (1990). The observation of the displacement of emulsifiers by confocal scanning laser microscopy. *Food Structure*, *9*, 305–316.

Jacobs, H., & Delcour, J. A. (1998). Hydrothermal modifications of granular starch, with retention of the granular structure: A review. *Journal of Agricultural Food Chemistry*, *46*(8), 2895–2905.

Kalichevsky, M. T., & Ring, S. G. (1987). Incompatibility of amylose and amylopectin in aqueous solution. *Carbohydrate Research*, *162*, 323–328.

Kalichevsky, M. T., Orford, P. D., & Ring, S. G. (1986). The incompatibility of concentrated aqueous solutions of dextran and amylose and its effect on amylose gelation. *Carbohydrate Polymers*, *6*, 145–154.

Koch, K., & Jane, J. L. (2000). Morphological changes of granules of different starches by surface gelatinization with calcium chloride. *Cereal Chemistry*, *77*(2), 115–120.

Li, L., Sosnowski, S., Chaffey, C. E., Balke, S. T., & Winnik, M. A. (1994). Surface morphology of a polymer blend examined by laser confocal fluorescence microscopy. *Langmuir*, *10*(8), 2495–2497.

Liu, Q., & Thompson, D. B. (1998). Effects of moisture content and different gelatinization heating temperatures on retrogradation of waxy-type maize starches. *Carbohydrate Research*, *314*, 221–235.

Mohammed, Z. H., Hember, M. W. N., Richardson, R. K., & Morris, E. R. (1998). Co-gelation of agarose and waxy maize starch. *Carbohydrate Polymers*, *36*, 37–48.

Niness, K. R. (1999). Inulin and oligofructose: What are they? *Journal of Nutrition*, *129*(7S), 1402S–1406S.

Pizzoli, M., Scandola, J., & Ceccorulli, G. (2002). Crystallization and melting of isotactic poly(3-hydroxy butyrate) in the presence of a low molecular weight diluent. *Macromolecules*, *35*, 3937–3941.

Roberfroid, M. B. (1999a). Caloric value of inulin and oligofructose. *Journal of Nutrition*, *129*, 1436S–1437S.

Roberfroid, M. B. (1999b). Concepts in functional foods: The case of inulin and oligofructose. *Journal of Nutrition*, *129*, 1398S–1401S.

Roberfroid, M. B. (2000). Prebiotics and probiotics: Are they functional foods? *American Journal of Clinical Nutrition*, *71*(6), 1682S–1687S.

Roberfroid, M., Gibson, G. R., & Delzenne, N. (1993). The biochemistry of oligofructose, a non-digestible fiber: An approach to calculate its caloric value. *Nutrition Review*, *51*(5), 137–146.

Rolee, A., & Le Meste, M. (1997). Thermomechanical behavior of concentrated starch–water preparations. *Cereal Chemistry*, *74*(5), 581–588.

Schaller-Povolny, L. A., & Smith, D. E. (1999). Sensory attributes and storage life of reduced fat ice cream as related to inulin content. *Journal of Food Science*, *64*(3), 555–559.

Sengupta, T., Razumovsky, L., & Damodaran, S. (2000). Phase separation in two-dimensional α-casein/β-casein/water ternary film at the air–water interface. *Langmuir*, *16*, 6583–6589.

Silva, R. F. (1996). Use of inulin as a natural texture modifier. *Cereal Foods World*, *41*(10), 792–794.

Stauffer, C. E. (2000). Emulsifiers as antistaling agents. *Cereals Food World*, *45*(3), 106–110.

Tolstoguzov, V. (2000). Foods as dispersed systems. Thermodynamic aspects of composition–property relationships in formulated food. *Journal of Thermal Analysis and Calorimetry*, *61*, 397–409.

Zimeri, J. E., & Kokini, J. L. (2002). The effect of moisture content on the crystallinity and glass transition temperature of inulin. *Carbohydrate Polymers*, *48*, 299–304.

Zimeri, J. E., & Kokini, J. L. (2003a). Phase transitions of inulin–waxy maize starch systems in limited moisture environments. *Carbohydrate Polymers*, *51*, 183–190.

Zimeri, J. E., Kokini, J. L (2003b). Rheological properties of inulin–waxy maize starch systems. Carbohydrate Polymers, in press.